Journal of Catalysis **185,** 192–198 (1999)
Article ID jcat.1999.2479, available online at http://www.idealibrary.com on IDEAL®

n-Hexane Reactions on EUROPT-1 at Different Hydrogen Pressures: The Possibility of Calculating Kinetic Parameters

Attila Wootsch and Zoltán Paál

Institute of Isotope and Surface Chemistry, Chemical Research Center of the Hungarian Academy of Sciences, Budapest P.O. Box 77, H-1525 Hungary

Received January 4, 1999; revised March 3, 1999; accepted March 3, 1999

Skeletal reactions of *n*-hexane on 6.3% Pt/SiO_2 (EUROPT-1) have been studied as a function of hydrogen pressure between 483 and 633 K. Turnover frequencies were calculated for the overall reaction as well as for individual processes, i.e., hydrogenolysis, isomerization, C_5-cyclization, and aromatization as well as dehydrogenation to hexenes. Curves with a maximum were observed for the conversion as a function of hydrogen pressure. Arrhenius plots could be calculated for constant hydrogen pressures as well as for maximum rates. The former lines "bend down" at higher temperatures. This may explain the different values determined in different experimental setups. Different straight Arrhenius lines were determined in the negative and in the positive hydrogen order range. We regard activation energies calculated at constant hydrogen pressures as "apparent" while those computed at the maximum rates may approximate "true" values. The apparent activation energies show compensation effect and give different compensation lines in the range of positive and negative hydrogen orders. In the case of bent Arrhenius plots, the computation resulted in *virtual isokinetic parameters*. Arrhenius parameters and compensation phenomena were determined for individual reactions, too. These results are in a good agreement with the mechanism suggested earlier for each reaction.

Key Words: ***n*-hexane transformation; turnover frequency; hydrogen pressure effect; compensation effect; virtual isokinetic parameters; Pt/SiO_2; EUROPT-1.**

INTRODUCTION

n-Hexane Reactions on EUROPT-1

EUROPT-1 is 6.3% Pt on silica studied extensively and can be regarded as a well-characterized "standard" platinum catalyst (1–5). Its reactivity in hydrocarbon transformations has been summarized by Bond *et al.* (2) who also reported values of turnover frequencies (TOF) for various hydrocarbon feeds, according to its classical definition, i.e., the number of transformed molecules per surface site per time unit (3). These results (2) were obtained in a single-pass reactor where the "time" was taken equal to the "contact time" defined as catalyst weight per mass flow rate W/F and the reaction rate as the ratio of conversion and contact time (4). Earlier studies from our laboratory reported how different mixtures of *n*-hexane and hydrogen react over EUROPT-1 in a closed loop reactor (5, 6). Different TOF values (2, 5, 6) and different activation energies (E_a) have been calculated from these two setups. A value of 117 kJ mol^{-1} was obtained for the overall conversion of *n*-hexane in a single pass reactor (2), while a value of around 65 kJ mol^{-1} could be calculated from the experiments in the closed loop reactor (5).

The variation of hydrogen pressure has a pronounced effect on the yields and selectivities on skeletal reactions of alkanes, the yields usually exhibiting maxima as a function of hydrogen pressure (5–10). These maxima are shifted toward higher hydrogen pressures as temperature increases (11–13). The influence of hydrogen pressure was found to be more marked at higher temperature and at higher pressure of *n*-hexane (5, 6).

The appearance of a maximum activity means that the hydrogen order of the reaction changed from positive to negative while the hydrogen pressure increased. The "landing-site model" by Frennet *et al.* (14, 15) provided one possible explanation for this phenomenon. They proposed a multiatomic "landing site" to be the active ensemble. This assumption results in maximum rates as a function of hydrogen pressure (14). Gault *et al.* (16a) adapted the multisite model to skeletal isomerization dividing the total rate expression into two parts: one depending on the hydrocarbon surface coverage, $g(\Theta_C)$, and the other depending on hydrogen coverage and partial pressure, $f\{\Theta_H^0, p(H_2)\}$. Summarizing this result when $f\{\Theta_H^0, p(H_2)\}$ prevails over $g(\Theta_C)$, the formal H_2 order is negative. On the other hand, if $g(\Theta_C)$ predominates over $f\{\Theta_H^0, p(H_2)\}$ the formal H_2 order is positive. They assumed that the "landing site" model described alkane reactions better than a simple dissociative chemisorption model (16b).

Bond *et al.* (17–19) have also found maximum types curves for *n*-butane hydrogenolysis over Ru/Al_2O_3 catalysts. Their phrasing of the explanation of this phenomenon is the most concise and precise so far (19). Accordingly, at lower H_2 pressures the (dissociatively chemisorbed) reactive intermediates require more hydrogen and that is why the reaction exhibits a positive hydrogen order. Having

0021-9517/99 $30.00

reached a certain H_2 pressure, the hydrogen coverage reaches a value optimum for the reaction corresponding to zero hydrogen order. Upon a further increase of $p(H_2)$, the reacting molecules have to compete with hydrogen for the empty surface sites. Hence, the reaction shows a negative hydrogen order (19). We assume that whenever negative or positive hydrogen orders were reported (16b, 20) the experiments may have been carried out in a pressure range outside of the range where the maximum value occurred.

The curves with a maximum for hydrogenolysis were approximated by the bimolecular Langmuir–Hinshelwood rate expression (21):

$$\text{rate} = k_1 K_A p_A K_B p_B / (1 + K_A p_A + K_B p_B)^2. \qquad [1]$$

Langmuir–Hinshelwood type rate equations were fitted for the hydrogen pressure dependence of ethane, propane, and *n*-butane hydrogenolysis also over Pt/Al_2O_3 (EUROPT-3) and $Pt–Re/Al_2O_3$ (EUROPT-4) (22). Other Langmuir–Hinshelwood type equations can be fitted to measure data of hydrogenolysis of ethane (22). If the rate limiting step is the reaction of an adsorbed hydrocarbon (A) with a hydrogen atom (B) then p_B should be replaced with $p_B^{0.5}$.

Compensation Effect

The linear correlation between the activation energy and the pre-exponential factor in heterogeneous catalysis is called the compensation effect. Compensation phenomena have been frequently reported either when the same reaction was studied on a series of different catalysts or when the same catalyst was used for different reactions (23). Bond discussed various cases of catalytic reactions; of the four case he described, one resulted in a "simple" compensation effect (24). Accordingly, Arrhenius plots that obey the compensation effect must intersect at exactly the same point defining an "isokinetic temperature" and "isokinetic rate" (24, 25). The isokinetic and compensation parameters are related to each other as follows (25):

$$\text{compensation effect: } \ln(A) = bE_a + c \qquad [2]$$

$$\text{isokinetic parameters: } T_{\text{iso}} = 1/(bR); \quad \ln(k_{\text{iso}}) = c \qquad [3]$$

There is no generally accepted interpretation for the compensation behavior. One possible explanation can be that the surface of the catalyst is energetically heterogeneous. Balandin published a formal equation for the energy, the free energy, and the entropy of adsorption for energetically heterogeneous surfaces and (26) obtained an equation similar to that used later by Galwey (25). The latter author suggested an exponential dependence between the partial constants and the activation energy. Similarly, if there is more than one type of active site on the catalyst surface, the fraction of the corresponding active site depends on the activation energy and gives rise to a compensation effect (25). Another kind of explanation is that the heat and entropy of adsorption are often related to each other in a linear manner (25), because a greater binding energy of the molecule to the surface strongly restricts their vibrational and rotational freedom.

Corma *et al.* (27) pointed out that the assumption of the transition state model of the compensation effect Eq. [2] means a linear relationship between enthalpy and entropy of the transition state. Karpinski and Larsson, in turn, correlated T_{iso} with the vibration frequency of the reactant molecule (28). If there is a complete resonance between the molecular vibration of the reactant and of the catalyst system, then $T_{\text{iso}} \approx 0.715\nu$, where ν is the vibration mode of the reactant molecule (expressed in cm^{-1}) that most strongly distorts the structure of the molecule toward the structure at the activated state (28). Rooney also derived the isokinetic parameter from the expanded Eyring equation (29). In his interpretation T_{iso} is correlated with k_{exp}, a rate-like characteristic frequency of the Arrhenius lines resulting in the compensation effect, as $k_{\text{exp}} = kT_{\text{iso}}/h$ if the conditions are standard (29).

The use of Langmuir–Hinshelwood kinetics can also lead to a compensation effect (25). Since the surface coverage of the catalyst by both hydrogen and reactive hydrocarbon intermediates changes significantly as temperature increases, the activation energy measured using constant hydrogen pressures can be regarded as "apparent" (E_{app}), while those based on constant surface coverage were labeled as "true" (E_t) (23). The compensation effect may occur because of the use of apparent rather than true kinetic parameters (23). Their relationship was defined by Temkin (30),

$$E_{\text{app}} = E_t + \Sigma n_i \Delta H, \qquad [4]$$

where n is the order of reaction and ΔH is the adsorption enthalpy.

Arrhenius plots measured at constant $p(H_2)$ were found to be "reversed" in some cases (31). This could be explained by the appearance of bell-shaped curves as a function of $p(H_2)$ (11, 12). Reversed Arrhenius plots were also reported for the hydrogenation of benzene on EUROPT-1 (2). Since the optimum hydrogen coverage requires higher and higher H_2 pressures as the temperature increases (5–8, 12, 13, 32), it might be more correct to measure the energy of activation at hydrogen pressure values that give maximum rates, i.e., when the hydrogen pressure order is zero (32). These values may differ from those determined at constant $p(H_2)$ (2, 5, 11).

The model reactions described so far (17–22) represented a single process, hydrogenolysis. *n*-Hexane, in turn, can undergo skeletal isomerization, C_5-cyclization to methylcyclopentane, and aromatization to give benzene (33–37), dehydrogenation to hexene accompanying these "skeletal" processes. This offers another challenge. All these

reactions may involve surface intermediates dehydrogenated to a different extent (8, 33) and/or various rate determining step(s) and the individual surface intermediate of the processes may compete not only with hydrogen but also with each other for free surface sites (8, 20, 33). We regard self-poisoning (5, 36, 37) as unimportant in the short runs applied here.

TOF and E_a values will be determined at maximum rates and compared with those obtained at constant hydrogen pressure. By doing so, we hope to succeed in resolving the apparent discrepancies that arise from the comparison of earlier papers using various setups and various conditions (2, 5, 6).

METHODS

The apparatus has been described in detail earlier (6). A closed loop reactor (volume ~70 ml) was filled with a mixture of *n*-hexane (nH) of 10 Torr (1.33 kPa) while the hydrogen pressure, $p(H_2)$, was varied between 60 and 480 Torr (8–64 kPa). The temperature ranged from 483 to 633 K. The same charge of catalyst (2.9 mg) was used, stabilized in several previous runs. Regeneration between runs was carried out with 30 Torr air for 2 min followed by evacuation and 3 min hydrogen treatment at 100 Torr. The sampling time was 5 min. Product analysis was performed gas chromatographically using a 50-m CP-Sil glass capillary column (5). The turnover frequencies (3) were calculated as the number of hexane molecules reacted per one surface Pt atom.

RESULTS

Figure 1 shows the yields of individual product classes at different temperature as a function of hydrogen pressure. Hydrogenolysis showed a positive hydrogen order, whereas the curves for benzene, methylcyclopentane (MCP), and skeletal isomers have maxima. The curves for the two latter closely related (38, 39) products resemble that for the hexane consumption (Fig. 2). Their sum is also shown in Fig. 1 as ΣC_6 saturated products.

Figure 2 shows the maximum curves for the overall consumption of *n*-hexane as a function of hydrogen pressure at different temperatures, starting from the lowest temperature where products appear (483 K) and ending where no maximum appeared any more (633 K). The apparent quality of our (spline-type) fitting and the resemblance of these curves to those constructed by computer simulation on the basis of the more correct Langmuir–Hinshelwood equation (23) permitted us to use as few hydrogen pressures as shown. The fitting shown in Fig. 2 is the best from all calculated Langmuir–Hinshelwood type fits. The maxima of the fitted curves are denoted by a "+" sign. They were shifted to higher hydrogen pressures with increasing temperature. The turnover frequencies calculated from the conversions of Fig. 2 are given in Tables 1 and 2. The underlined numbers in Table 1 have been calculated from the encircled experimental points of Fig. 1. The data in Table 2, in turn, belong to the maxima of the curve fitted to the "+" signs in Fig. 2 by a mathematical procedure.

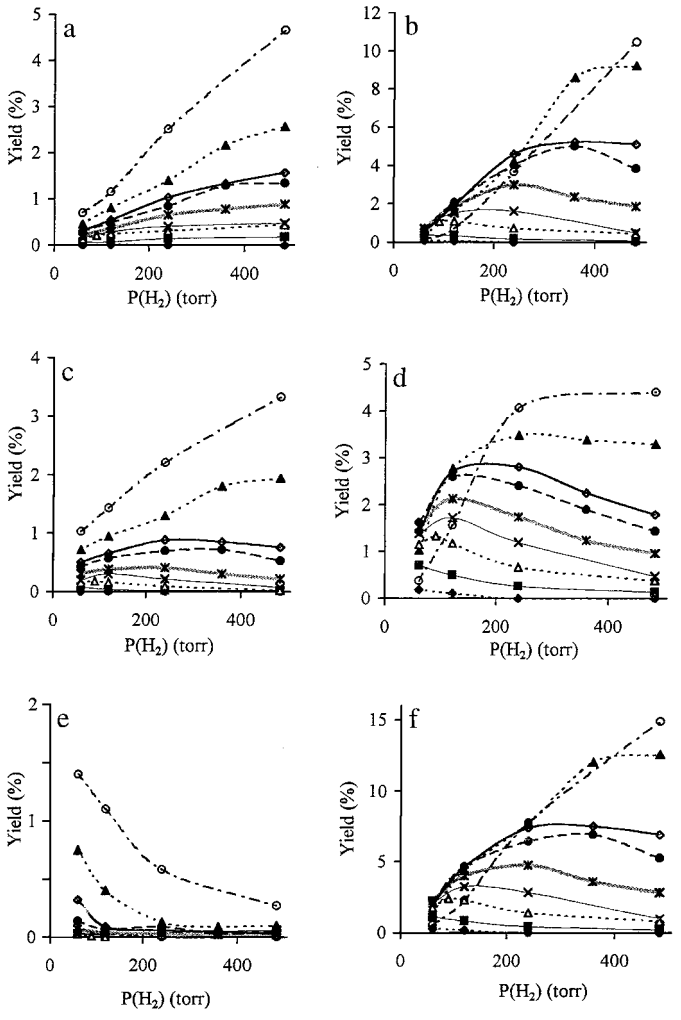

FIG. 1. Yields of various products as a function of hydrogen pressure at different temperature. (a) $<C_6$ products; (b) skeletal isomers; (c) benzene; (d) MCP; (e) hexenes; (f) sum of C_6 saturated products. ◆, 483 K; ■, 513 K; △, 533 K; ×, 543 K; ∗, 558 K; ●, 573 K; ◇, 583 K; ▲, 603 K, ○, 633 K.

Figure 3 shows the activation energies calculated from the maximum points. The values belonging to the two kinds of maxima (measured and fitted) were very close, 65 and 66 kJ/mol, respectively, well within the expected range of experimental error. Thus, these E_a values might not be very sensitive to the *exact* position of maxima, as seen from the curve shapes in Fig. 2. This indicated that the use of relatively few $p(H_2)$ values could give rise to a negligible error only.

Arrhenius plots calculated at constant hydrogen pressures and at maximum rates, respectively, are presented in Fig. 4. The "bending" of Arrhenius lines is obvious, even

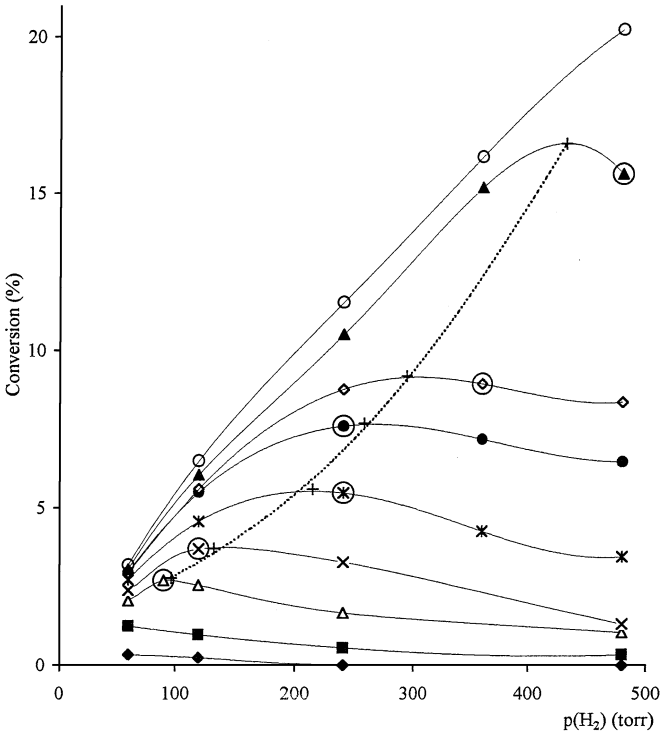

FIG. 2. Conversion (%) of *n*-hexane transformation over EUROPT-1 at different temperatures. The curves represent a closest fit (spline) curve. Encircled points are the measured ones that are nearest to maxima. The dotted line is a second-order polynom for determining the maxima of the individual curves. This is a mathematical procedure with no particular chemical meaning. ◆, 483 K; ■, 513 K; Δ, 533 K; ×, 543 K; ∗, 558 K; ●, 573 K; ◇, 583 K; ▲, 603 K; ○, 633 K.

if their "inversion" (31) has not been reached. The Arrhenius line calculated from the maxima defined practically an enveloping curve connecting the break points, except for the lowest hydrogen pressure (5, 36, 37). Two different Arrhenius lines are shown at constant hydrogen pressure:

TABLE 1

Turnover Frequencies (TOF in h^{-1}) for *n*-Hexane Transformation over EUROPT-1

	$p(H_2)$ (Torr)				
T (K)	60	120	240	360	480
483	2.7	1.9			
513	10.1	7.9	3.8		2.7
533	16.7	20.7	13.5		8.4
543	19.3	30.1	26.6		10.7
558	22.1	37.1	44.5	34.7	28.1
573	24.0	44.7	61.8	66.8	52.7
583	23.8	45.6	71.3	72.8	68.2
603	24.7	49.2	85.4	124.4	127.2
633	25.9	52.8	93.7	131.6	164.5

Note. Underlined letters are the encircled points from Fig. 1 for each temperature.

TABLE 2

H_2 Pressures for the Maximum Rates and the Corresponding TOF Values (+ from Fig. 2)

T (K)	$p(H_2)$ (Torr)	TOF (h^{-1})
533	97	22.5
543	133	30.1
558	214	45.5
573	257	62.5
583	294	74.7
603	432	135.0

one in the negative and one in the positive hydrogen order range. As the Temkin equation (Eq. [4]) predicts, with the change of n_H from negative to positive, the apparent activation energy must also change.

The corresponding apparent Arrhenius parameters can be seen in Table 3. (These are mathematically calculated parameters of the measured Arrhenius plots, and those in the range of positive hydrogen order may have no physicochemical reality.) The values at the highest $p(H_2)$ are in a good agreement with those measured by Ponec *et al.* for *n*-hexane (2, 4, 40) and also with the more general conclusion (23) that working at the highest hydrogen pressures results in high E_{app}, low rates, and negative hydrogen order (n_H). By definition, the fastest rates appeared where n_H was close to zero. Here the E_{app} was lower. As predicted from Eq. [4], the apparent energy is independent of ΔH_H for the points calculated from the maximum where $n_H = 0$, but depends on ΔH_{nH} and n_{nH}. The value of n_{nH} changed from one to zero; at the same time it depended on the temperature and on the hydrogen pressure (10). From the results reported earlier (hydrogen pressure, 120 Torr, the temperature range between 543 and 633 K, with $n_{nH} \approx 1$ at 1.33 kPa (10)) we estimate a value for n_{nH} close to unity in our range of

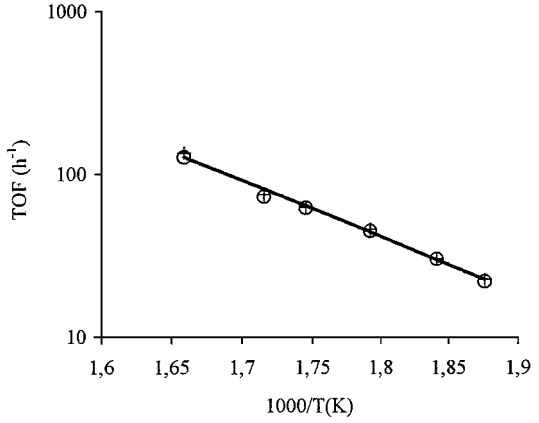

FIG. 3. Arrhenius plot calculated from maximum values of the curves in Fig. 2. $E_a = 66$ kJ/mol ($R^2 = 0.98$). +, points from the fitted polynom; ○, points from the encircled points.

TABLE 3

Arrhenius Parameters Calculated from Fig. 4

H_2 order	$p(H_2)$ (torr)	E_a (kJ mol^{-1})	ln A (h^{-1})
Positive	60	8	4.9
	120	13	6.4
	240	17	7.8
Zero	Peak	66	18.0
Negative	60	91	23.7
	120	102	26.0
	240	115	28.1
	480	117	28.3

measurements. Hence, the activation energy obtained from peak points is $E_{\text{maximum}} \approx E_t + \Delta H_{n\text{H}}$. We had insufficient data to calculate the actual value of $\Delta H_{n\text{H}}$, which could be calculated successfully for Ni catalysts by Tétényi (41). The calculated values can be regarded as close to "true" values if we apply one single Temkin equation [4] for the overall reaction. However, this is a rough approximation. Different reactions leading to each product class have their own elementary steps and surface intermediates. Their formal description involves individual Langmuir-type equations [1], the three constants (k_1, K_A, K_B) of which show their own temperature dependence. Thus, the E_a calculated may eliminate *some* but not *all* distorting factors and may be closer to the "true" value but not identical to it.

The curves with a maximum for the overall reaction and those for some products (Figs. 1 and 2) being similar, we could calculate the apparent E_a at constant hydrogen pressures, as well as from the "peak points" for each product, in a way analogous to the overall reaction. These values are also apparent because the variation of hydrogen coverage of the surface with $p(H_2)$ and temperature influences the rates of individual reaction routes in a different way (Table 4).

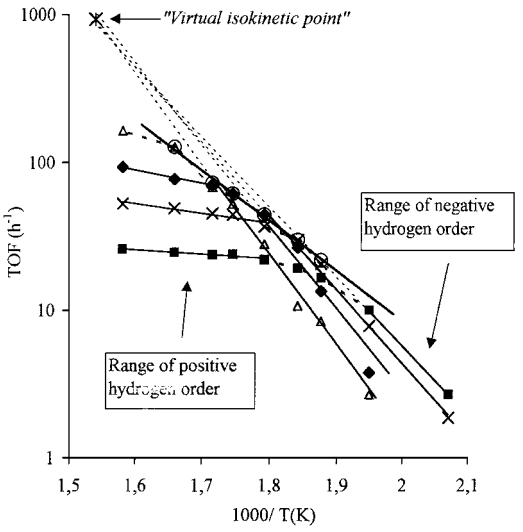

FIG. 4. Arrhenius plots calculated at constant hydrogen pressures $p(H_2)$. Encircled points correspond to maximum of conversion (Fig. 2). △, 480 Torr; ◆, 240 Torr; ×, 120 Torr; ■, 60 Torr.

DISCUSSION

Turnover Frequencies Determined under Different Conditions

The different E_a values reported (2, 5, 6) can be explained on the basis of Fig. 4. The temperature was between 484 and 518 K, the H_2 pressure was (a constant) 0.94 atm (95.2 kPa), and the pressure of *n*-hexane 0.059 atm (5.97 kPa) in Ref. (2). Those results obtained at high hydrogen pressure should, therefore, correspond to the region of negative hydrogen order. The reported value of 117 kJ/mol (2) agrees well with our value of 117 kJ/mol measured at 480 Torr (64 kPa).

The reaction rates under the given conditions represent an objective fact of nature. We use, however, an imperfect

TABLE 4

Apparent Arrhenius Parameters of Various Products (E_a in kJ mol^{-1}, A in h^{-1})[a]

		Benzene		Isomer		MCP		Sum. C_6 saturated	
H_2 order	$p(H_2)$	E_a	ln(A)	E_a	ln(A)	E_a	ln(A)	E_a	ln(A)
Negative	60		—		—		—	89	23.0
	120		—	101	24.8		—	104	26.4
	240	140	30.1	130	31.0	84	20.7	112	27.6
	480	147	32.0	135	31.5	90	21.4	124	29.8
Zero	Peak		—	90	22.3	44	12.1	65	17.5
Positive	60	51	11.9		—		—		—
	120	51	12.1		—		—		—
	240	57	13.7		—		—		—
	480	57	13.8		—		—		—

[a] No Arrhenius plots could be fitted for spaces marked with —.

human approach when approximating with a mathematical formula including sometimes arbitrary values. The actual result depends on the approximation selected. The present TOF values were larger than those reported in the literature (2) but they are close to our earlier values obtained in the same setup loaded with more EUROPT-1 (5). Various reasons may cause this difference. We used a value of 60% dispersion (3) whereas a dispersion of 100% was used earlier (2). This alone resulted in our TOF values being higher by a factor 1.6. Further and more pronounced differences can be caused by using various assumptions as a basis of calculation. The actual calculated values are not independent of the experimental setup used. We used a closed loop reactor where a "run-in" period was reported (10). Hence, the apparent rate at $t=0$ is *lower* than after a certain reaction time and the tangent at $t=0$ does not represent the rate of steady-state transformation. We calculated rates from the near-linear part of the conversion-time curves. Apart from uncertainties in determining the number of active sites, taken equal to the number of surface Pt atoms determined earlier (1c), another uncertainty arises from the arbitrary definition of the reaction time in different experimental setups (2, 5). We wrote the total length of the run in the denominator of the TOF equation for the closed loop reactor whereas the "contact time" in the single-pass reactor was defined as the ratio of catalyst weight per mass flow rate, W/F (4). The first case disregards the fact that not all molecules would be in contact simultaneously with the catalyst, whereas the second assumption cannot consider the number of molecules that just pass over the catalyst bed without reacting on or even contacting the active surface (40). This obviously leads to lower TOF values in the latter case (2). It was possible to determine the real time of sojourn of the molecules on the active surface by using the isotope tracer method (42). A similar measurement in our case could resolve the above apparent discrepancy.

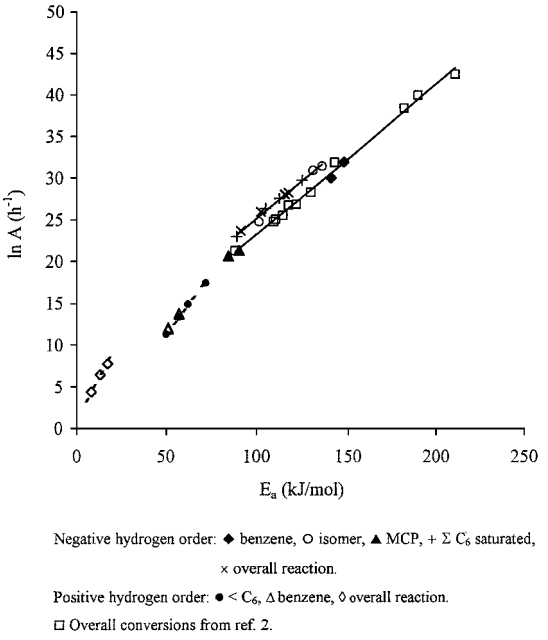

FIG. 5. The compensation effect for *n*-hexane conversion as well as for individual reactions. Earlier results of several reactions on EUROPT-1 (2) are compared with those of present work. Negative hydrogen order: ◆, benzene; ○, isomer; ▲ MCP, $+\Sigma C_6$ saturated; ×, overall reaction. Positive hydrogen order: ●, $<C_6$; ▲, benzene; ◇, overall reaction; □, overall conversions from Ref. (2).

Compensation Effects

Figure 5 compares our results with the compensation line published earlier (2). The points of the overall reaction calculated in the negative hydrogen order range determine a straight line parallel to that taken from the literature but lie at higher values. Arrhenius parameters were calculated in the region of negative hydrogen order for MCP, for skeletal isomers, for benzene, and for the ΣC_6 saturated products. The same was done in the region of positive hydrogen order for the overall process, hydrogenolysis, and benzene (Fig. 5). The slopes of the compensation lines for the negative and positive hydrogen order ranges were different. Further, some points for different reactions lie on the same compensation line, while others are different. In particular, (a) benzene and MCP agree well with each other and also coincide with the line reported earlier (2); (b) skeletal isomers and the ΣC_6 saturated products agree with those of the *n*-hexane consumption (the higher parallel line); and (c) the data points for hydrogenolysis lie on a different curve coinciding with that of aromatization in the positive hydrogen order range.

Arrhenius plots that obey the compensation effect ought to intersect each other at exactly the same point defining thus an isokinetic temperature and isokinetic rate (24, 25). But Arrhenius lines have calculated at different pressures cannot intersect each other at the same point because if they do so there must be a temperature where reaction rate was totally independent of the pressure (23). The isokinetic parameters calculated for the overall process are $T_{iso} \cong 650$ K, $k_{iso} \cong 850$ h^{-1} in the range of negative hydrogen order and $T_{iso} \cong 320$ K, $k_{iso} \cong 5$ h^{-1} in the positive range. The Temkin equation [4] predicts that reactions in the same range of hydrogen order can only be compared. In the case of bent Arrhenius plots, their existence of an intersection is a mathematical possibility rather than a physicochemical reality. They obey the "simple" compensation effect (24) but, since the intersection points are out of the range of the real experimental data, they can be regarded as *virtual isokinetic parameters*. This agrees with the statement that the compensation effect is a linear relationship between the pre-exponential factor and activation energy giving isokinetic parameters but it is not sure that they exist in the feasible range of experimental conditions (21, 23, 27).

Possible Active Sites

Accepting the cubooctahedron model of EUROPT-1 (43), different reactions were attributed to corner atoms, the (100) plane, and the (111) plane (10). The formation of skeletal isomers, C_6 saturated products being on the same compensation line as the overall conversion (Fig. 5), may mean that these closely related reactions (38, 39) determine the overall rate of *n*-hexane transformations in the range of the negative hydrogen order, i.e., when hydrogen is abundant (21). It is not excluded that their active site involves some Pt–H ensembles (6, 13, 16, 44). These assumptions are complementary rather than mutually incompatible. The first step for each reaction can be a (rate determining (45)) dissociation of the first C–H bond of the saturated reactant. Various surface intermediates can be formed from this starting adspecies (37). Hydrogen-rich conditions favor the formation of C_6 saturated products. Their common adsorbed C_5-cyclic intermediate (38, 39) can desorb as MCP or form isomer products. The compensation curve (Fig. 4) of aromatization coincides with hydrogenolysis, both requiring assumedly intermediates with several C–H bonds broken (8, 33, 46).

CONCLUSION

Our results confirm the qualitative validity of earlier ideas (17–22) for the interpretation of maxima as a function of $p(H_2)$ for hydrogenolysis for the complex reaction of *n*-hexane, too, although the maximum curves could not be fitted with a single Langmuir–Hinshelwood equation. We believe that an adequate explanation was given how and why the numerical values of E_a and TOF measured under different conditions differ from each other.

ACKNOWLEDGMENTS

The authors thank Professors G. C. Bond and V. Ponec for valuable discussion and advice in comparing present and published results as well as for permitting access to still unpublished papers. Financial support from the Hungarian National Science Foundation Grant OTKA T 25599 is gratefully acknowledged.

REFERENCES

1. (a) Bond, G. C., and Wells, P. B., *Appl. Catal.* **18**, 221 (1985); (b) Bond, G. C., and Wells, P. B., *Appl. Catal.* **18**, 225 (1985); (c) Geus, J. W., and Wells, P. B., *Appl. Catal.* **18**, 231 (1985); (d) Frennet, A., and Wells, P. B., *Appl. Catal.* **18**, 243 (1985); (e) Wells, P. B., *Appl. Catal.* **18**, 289 (1985).
2. Bond, G. C., Maire, G., and Garin, F., *Appl. Catal.* **41**, 313 (1988).
3. Boudart, M., *in* "Handbook of Heterogeneous Catalysis" (G. Ertl, H. Knözinger, and J. Weitkamp, Eds.), Vol. 3, p. 958. Verlag Chemie, Weinheim, 1997.
4. Ponec, V., *in* "Electronic Structure and Reactivity of Metal Surfaces" (E. G. Derouane and A. A. Lucas, Eds.), p. 537. Plenum Press, New York, 1976.
5. Paál, Z., Groeneweg, H., and Paál-Lukács, J., *J. Chem. Soc. Faraday Trans.* **86**, 3159 (1990).
6. Paál, Z., Groeneweg, H., and Zimmer, H., *Catal. Today* **5**, 199 (1989).
7. Paál, Z., and Tétényi, P., *Dokl. Akad. Nauk SSSR* **201**, 1119 (1971).
8. Paál, Z., *Adv. Catal.* **29**, 273 (1980).
9. Zimmer, H., Dobrovolszky, M., Tétényi, P., and Paál, Z., *J. Phys. Chem.* **90**, 4758 (1986).
10. Bond, G. C., and Paál, Z., *Appl. Catal.* **86**, 1 (1992).
11. Paál, Z., *J. Catal.* **91**, 181 (1985).
12. Paál, Z., and Somorjai, G., *in* "Handbook of Heterogeneous Catalysis" (G. Ertl, H. Knözinger, and J. Weitkamp, Eds.), Vol. 3, p. 1084. Verlag Chemie, Weinheim, 1997.
13. Paál, Z., *in* "Hydrogen Effects in Catalysis" (Z. Paál and P. G. Menon, Eds.), p. 449. Dekker, New York, 1988.
14. Frennet, A., Lienard, G., Crucq, A., and Degols, *J. Catal.* **53**, 150 (1978).
15. Frennet, A., *in* "Hydrogen Effects in Catalysis" (Z. Paál and P. G. Menon, Eds.), p. 399. Dekker, New York, 1988.
16. (a) Gault, F. G., Amir-Ebrahimi, V., Garin, F., Parayre, P., and Weisang, F., *Bull. Soc. Chim. Belg.* **88**, 475 (1979); (b) Parayre, P., Amir-Ebrahimi, V., Gault, F. G., and Frennet, A., *J. Chem. Soc. Faraday Trans.* **76**, 1704 (1980).
17. Bond, G. C., and Slaa, J. C., *J. Mol. Catal.* **89**, 221 (1994).
18. Bond, G. C., and Slaa, J. C., *Catal. Lett.* **23**, 293 (1994).
19. Bond, G. C., and Slaa, J. C., *J. Mol. Catal.* **98**, 81 (1995).
20. Garin, F., and Gault, F. G., *J. Am. Chem. Soc.* **97**, 4466 (1975).
21. Bond, G. C., Hooper, A. D., Slaa, J. C., and Taylor, A. O., *J. Catal.* **163**, 319 (1996).
22. Bond, G. C., and Cunningham, R. H., *J. Catal.* **166**, 172 (1997).
23. Bond, G. C., *Catal. Today* **49**, 41 (1999).
24. Bond, G. C., "Catalysis by Metals," p. 139. Academic Press, London/New York, 1962.
25. Galwey, A. K., *Adv. Catal.* **26**, 247 (1977).
26. Balandin, A. A., *Dokl. Akad. Nauk SSSR* **93**, 55 (1953).
27. Corma, A., Lopis, F., Monton, J. B., and Weller, S., *J. Catal.* **142**, 97 (1993).
28. Karpinski, Z., and Larsson, R., *J. Catal.* **168**, 532 (1997).
29. Rooney, J. J., *J. Mol. Catal.* **129**, 131 (1998).
30. Temkin, M., *Acta Physicochim. URSS* **3**, 312 (1935).
31. Davis, S. M., Zaera, M., and Somorjai, G., *J. Catal.* **85**, 206 (1984).
32. Paál, Z., Matusek, K., and Tétényi, P., *Acta Chim. Acad. Sci. Hung.* **94**, 119 (1977).
33. Paál, Z., Székely, G., and Tétényi, P., *J. Catal.* **58**, 108 (1979).
34. Ponec, V., and Bond, G. C., "Catalysis by Metals and Alloys." Elsevier, Amsterdam, 1995.
35. Menacherry, P. V., and Haller, G. L., *J. Catal.* **177**, 175 (1998).
36. Fukunaga, T., and Ponec, V., *Appl. Catal. A* **154**, 207 (1997).
37. Paál, Z., Xu, X. L., Paál-Lukács, J., Vogel, W., Muhler, M., and Schlögl, R., *J. Catal.* **152**, 252 (1995).
38. Maire, G., Plouidy, G., Prudhomme, J. C., and Gault, F. G., *J. Catal.* **4**, 556 (1965).
39. Barron, Y., Maire, G., Muller, M., and Gault, F. G., *J. Catal.* **5**, 428 (1966).
40. Ponec, V., personal communication.
41. Tétényi, P., *React. Kinet. Catal. Lett.* **53**, 369 (1994).
42. Norval, S. V., and Thomson S. J., *J. Chem. Soc. Faraday Trans.* **75**, 1798 (1979).
43. Gnutzmann, V., and Vogel, W., *J. Phys. Chem.* **94**, 4991 (1990).
44. Bragin, O. V., Olferyeva, T. G., Preobrazensky, A. V., Liberman, A. L., and Kazansky, B. A., *Dokl. Akad. Nauk SSSR* **202**, 339 (1972).
45. Tétényi, P., *Acta Chim. Acad. Sci. Hung.* **40**, 157 (1964).
46. Paál, Z., and Tétényi, P., *in* "Catalysis Specialist Periodical Reports" (G. C. Bond and G. Webb, Eds.), Vol. 5, p. 80. The Royal Society of Chemistry, London, 1982.